# Recoil Proton Polarization from 225-Mev $\pi^-$-$p$ Scattering*†

J. F. KUNZE,‡ T. A. ROMANOWSKI, J. ASHKIN, AND A. BURGER§

*Carnegie Institute of Technology, Pittsburgh, Pennsylvania*

(Received August 11, 1959)

$\pi^-$ mesons of energy 225 Mev were scattered from liquid hydrogen. The polarization of the recoil proton has been measured at two angles. For analyzing the polarization, a counter controlled cloud chamber was used. Recoil protons, which experienced scatterings in a carbon plate of the cloud chamber, were photographed stereoscopically. The pictures were later projected, and the necessary measurements of the scattering were made directly in three dimensions. The computed polarizations are $-0.13\pm0.16$ at a laboratory recoil angle of 15°, and $+0.36\pm0.29$ at 31°. The positive sign is for polarization in the direction of the vector cross product of the incident pion momentum and the recoil proton momentum. A comparison of the data is made with various sets of scattering phase shifts which represent the differential cross-section data equally well. The results favor the Orear type of Fermi set in which the $S$-wave $\alpha_1$ phase shift is positive.

## I. INTRODUCTION

IT has been known for a long time that the problem of extracting a set of scattering phase shifts from the experimental data on cross sections for pion-proton scattering does not, in general, have a unique solution. Of the several possibilities in the energy range below 250 Mev, there are strong theoretical reasons for preferring solutions of the Fermi type which are characterized by a resonance in the $p$ state of total angular momentum $\frac{3}{2}$ and isotopic spin $\frac{3}{2}$. Above 200 Mev, however, it was noticed by Orear[1] that the differential cross sections could be equally well represented by two solutions of the Fermi type: type (i) characterized by a positive phase shift $\alpha_1$ (for the $s$-state of isotopic spin $\frac{1}{2}$) varying approximately linearly with the pion momentum; and type (ii) in which $\alpha_1$ is negative, having changed in sign at about 170 Mev. The measurements of Ashkin et al.[2] at 220-Mev pion kinetic energy confirm such possibilities. If in addition we allow solutions of the type first discovered by Yang,[3] the ambiguity is doubled. However, these solutions have a much less plausible energy dependence for the large phase shifts.[4,5]

As a means of distinguishing one phase-shift solution from another, Fermi[6] proposed supplementing the

measurements of the angular distribution in the scattering with a measurement of the polarization of the nucleon which recoils. A nonvanishing polarization can in general be expected because of the strong spin-dependence in the scattering. For illustration, consider the elastic scattering of negative pions by protons at 220 Mev. Figure 1 shows the (theoretical) polarization as a function of proton laboratory angle, calculated according to Appendix II, for the pair of Fermi type phase-shift solutions (i) and (ii) and the associated solutions of the Yang type.

In the meantime, development of the dispersion relations for pion-nucleon scattering provided a powerful argument against the Yang phase shifts.[7,8] The ambiguity with respect to the Fermi solutions (i) and (ii) still persisted, however.[9] For this reason it was considered useful to continue with the measurement of the proton polarization.
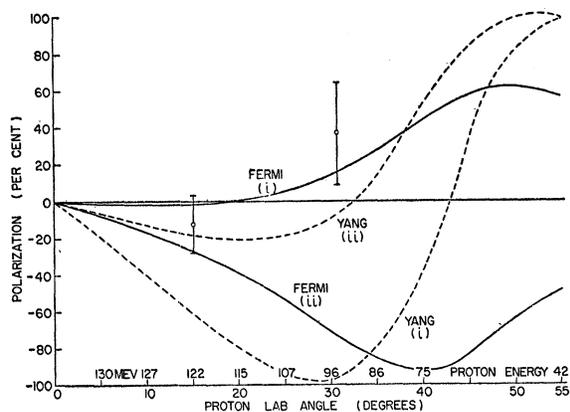


FIG. 1. Theoretical polarization for the recoil proton in $\pi^-$-$p$ scattering for four different phase shift sets, and the experimental results.

[1] J. Orear, Phys. Rev. 100, 288 (1955).

[2] Ashkin, Blaser, Feiner, and Stern, Phys. Rev. 105, 724 (1957).

[3] C. Yang (private communication to E. Fermi); and H. A. Bethe and F. de Hoffmann, *Mesons and Fields* (Row, Peterson and Company, Evanston, 1955), Vol. 2, p. 72.

[4] A further complication comes from the observation of Minami that it is possible to exchange the phase shifts for $l=j+\frac{1}{2}$ with those for $l=j-\frac{1}{2}$ without changing the cross section. Solutions of this type are very unlikely since they introduce abnormally large $d$-wave phase shifts in an energy range where only $s$ waves and $p$ waves are expected to be appreciably scattered. Furthermore this set does not satisfy the dispersion relations (see reference 8).

[5] S. Minami, Progr. Theoret. Phys. (Kyoto) 11, 213 (1954).

[6] E. Fermi, Phys. Rev. 91, 947 (1953).

[7] W. C. Davidon and M. L. Goldberger, Phys. Rev. 104, 1119 (1956); also W. Gilbert and G. Screaton, Phys. Rev. 104, 1758 (1956).

[8] S. J. Lindenbaum and R. Sternheimer, Phys. Rev. 110, 1174 (1958).

[9] An argument favoring positive $\alpha_1$, has recently been given by A. Stanghellini, Nuovo cimento 10, 398 (1958).

The measurements to be considered below have been performed at $224\pm10$ Mev, corresponding very nearly to the energy of the differential cross-section measurements of Ashkin et al. To distinguish between the two Fermi type solutions it is necessary to observe the $\pi^-$ scattering since it involves the state of isotopic spin $\frac{1}{2}$ as well as $\frac{3}{2}$. The corresponding measurement of polarization in the $\pi^+$ scattering (pure $I=\frac{3}{2}$) was not possible with the weak $\pi^+$ beam available.

Figure 1 shows that at angles up to 40° there is a large polarization difference between all but the Fermi (i) and Yang (ii) phase-shift sets. A significant difference does exist between these two sets at a proton angle of 50°. At this angle, the proton energy is so low that a convenient polarization analyzing material is difficult to find. It was decided to restrict the measurements to protons recoiling at angles of not more than about 30° in the laboratory, so that the proton energy would be sufficiently large to permit the use of carbon as an analyzing material. In practice the measurements were made for protons recoiling at 15° and 31° in the laboratory.

## II. EXPERIMENTAL ARRANGEMENT

A measurement of the polarization of the recoil proton requires looking for an azimuthal asymmetry in a subsequent scattering of the proton by a suitable polarization analyzer. The essential steps are indicated in Fig. 2, showing the incident and scattered pion, the recoil proton with its direction of polarization, and the subsequent scattering of the proton by the analyzer, which in this case is a carbon target. Assuming the conservation of parity in the pion-nucleon interaction, the axial vector representing the polarization of the recoil proton must necessarily be parallel to the only axial vector which is defined by the primary collision, namely the vector cross product of the initial and final momentum for either pion or proton. The proton polarization is therefore perpendicular to the plane defined by the scattered pion and the recoil proton momenta. The magnitude of the polarization, $P$, is to be determined from the angular distribution in the collision with the carbon analyzer according to the cross section

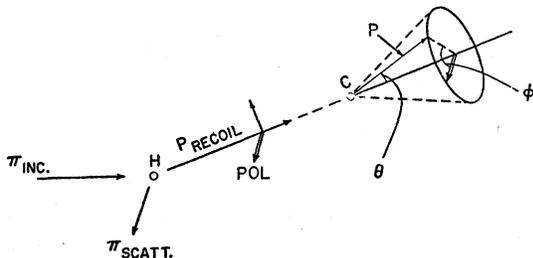$$\sigma(\theta,\phi,E)=\sigma_0(\theta,E)[1+PP_c(\theta,E)\sin\phi]. \quad (1)$$



FIG. 2. Method of measuring recoil proton polarization.

In this expression, $P_c(\theta,E)$ is the analyzing power of carbon for collisions in which protons of energy $E$ are deflected through an angle $\theta$ (see Fig. 2), $\phi$ is the azimuthal angle of the scattered proton measured from the incident polarization direction, and $\sigma_0(\theta,E)$ is the scattering cross section for unpolarized protons.

The conventional polarization experiments, where proton beams of high intensity are available, use counters to compare the counting rates for scattering at $\sin\phi=+1$ and $\sin\phi=-1$ (left-right asymmetry) for various scattering angles $\theta$. Unfortunately, for this recoil nucleon experiment, the limited intensity of the pion beam (about 100 cm$^{-2}$ sec$^{-1}$) makes it prohibitively difficult to use counters to detect the asymmetry in the proton scattering. With this intensity, and a reasonable geometry, one could only expect a number of recoil protons of the order of a thousand per hour incident on the carbon target. It was therefore necessary to find a method of detection having a large available solid angle and at the same time giving good accuracy in the determination of the angles of the proton scattering, $\theta$ and $\phi$. Because of the strong variation of $P_c(\theta,E)$ with proton energy in the range of interest from 130 Mev to 60 Mev, it would be useful if the proton energy could also be estimated for each scattering event. For these reasons, we have chosen a visual technique employing a counter-controlled expansion cloud chamber in which the protons are scattered by a carbon analyzer. The scatterings are photographed stereoscopically.

### 1. Pion Beam

The negative pions were produced in a target inside the Carnegie Tech cyclotron. The meson beam was focused by two quadrupole magnets mounted on the cyclotron coil can. After passing through the 12-ft shielding wall, mesons of the proper momentum were chosen by bending the beam 40° with a selecting magnet. The resultant beam had an intensity of 100 pions cm$^{-2}$ sec$^{-1}$, and a mean energy of $224\pm10$ Mev at the center of the liquid hydrogen target. The hydrogen was confined to a 2-in.$\times4\frac{3}{4}$-in.$\times4\frac{3}{4}$-in. channel inclined to the meson beam at approximately the same angle as the cloud chamber (Fig. 3). The target was constructed of styrofoam and had a loss rate of approximately 0.4 liter per hour.

### 2. Counter System

The counter arrangement consisted of six plastic scintillators (Fig. 3). The meson beam was monitored by two $2\frac{3}{4}$-in.$\times2\frac{3}{4}$-in. counters, 1 and 2, before entering the hydrogen target. The back scattered meson was counted by counter number 3 which was 8 in.$\times9$ in. The recoil proton entered a counter telescope consisting of two counters, number 4 and 5, each 4 in.$\times1\frac{3}{4}$ in. and $\frac{3}{16}$ in. thick. Counter number 5 was imbedded in a carbon plate located inside the cloud chamber. A large 16-in.$\times6\frac{1}{2}$-in. anticoincidence counter was placed be-

hind the cloud chamber to assure that the proton entering the cloud chamber would not be photographed unless it missed the anticoincidence counter, hereafter called the AC counter.

The target, serving as the polarization analyzer, is located in the center of the cloud chamber and consists of $\frac{5}{8}$ in. of carbon (density 1.55 g/cm³), followed by $\frac{3}{16}$ inch of scintillant [(CH)$_n$, density 1.0 g/cm³]. The scintillant area is 4 in.$\times 1\frac{3}{4}$ in. A Lucite light pipe leads through an airtight seal to a photomultiplier tube outside the cloud chamber. Initially, the scintillant was placed at the entrance side of the carbon, but was later reversed so that it came after the carbon scatterer. This change was made to reduce the number of events containing protons that stopped in the carbon after counting in the scintillant. Counter 4 was placed just outside of the cloud-chamber wall and the distance between counter 4 and 5 was about 6 in. The AC counter was 21 in. behind the back cloud-chamber wall. Efficiency of all of the counters was checked in the meson and proton beams and was determined to be about 100% in each case.

Because of the intense beam necessary, the general room background flooded the cloud chamber with electron tracks. To minimize this effect, 4-ft thick concrete shielding was placed near and around the cloud chamber. The recoil meson counter was also carefully shielded from any direct scattering from the incident beam.

## 3. Cloud Chamber

The cloud chamber is constructed of stainless steel with the walls reduced to a thickness of $\frac{1}{32}$ in. where the beam enters and leaves the chamber. The top and two sides are $\frac{1}{2}$-inch thick glass windows. The entire bottom of the chamber is a rubber diaphragm. The inside chamber dimensions are 9 in.$\times 9$ in. by $4\frac{1}{2}$ in. high. The atmosphere was argon, saturated with a 60/40 ethyl alcohol-water mixture. A pool of about 15 cm³ was allowed to remain on top of the diaphragm. To prevent moisture accumulation on the glass windows, a nickel plated grid of copper tubes was placed just
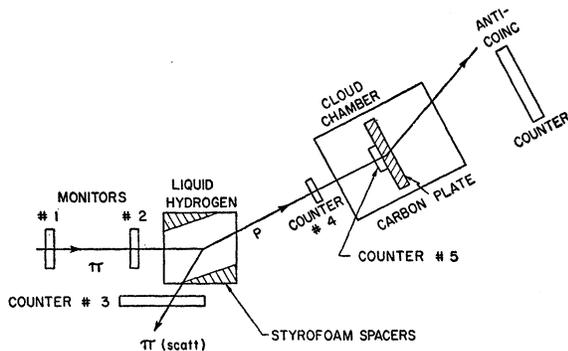
above the diaphragm and covered with black velvet, which served as a photographic background. Water, a few degrees cooler than the cloud-chamber walls, flowed through the grid, thus keeping the atmosphere slightly below saturation and preventing condensation on the walls.

A clearing field, averaging 80 v/cm, was applied to the cloud chamber. The walls and carbon plate were grounded, and the voltage was carried by two wire grids spaced midway between the carbon plate and cloud-chamber walls. The field was sufficient to clear the chamber of ions in the 5-milliseconds interval between cyclotron beam pulses.

Initially the cloud chamber was operated with a fast overcompression immediately following the expansion.[10] This operation cycle proved to be unsuccessful. However, when the diaphragm was allowed to remain in the expanded position long enough for the fog droplets to precipitate, the overcompression then served the purpose of quickly returning the chamber to thermal equilibrium. The chamber was expanded rapidly and allowed to remain in the expanded condition for 15 seconds. The overcompression and after-expansion required about 2 seconds. The chamber could be recycled every 25 seconds and still maintain satisfactory track conditions. In practice, the usual triggering rate was approximately once every $2\frac{1}{2}$ minutes, depending on the beam. The overcompression cycle seemed to have the desirable effect of hastening the time required to clear a fogged chamber, resulting from an overexpansion, or an expansion while the chamber was flooded with ions. Such a cleaning operation was completed in about 5 cycles, but would require at least 10 minutes by ordinary slow expansion methods.

The chamber was usually operated with an ambient temperature of 68°F, maintained by an air conditioning system. However, a satisfactory operating range was found to be 60° to 75°F. The tracks seemed to suffer no degeneration throughout this range if the expansion ratio was properly adjusted.

The sequence of operations necessary to record an event is outlined as follows: The scintillation counter coincidence circuit triggered a discriminator which immediately turned off the chamber clearing field and the cyclotron, and released the pressure under the cloud-chamber diaphragm, allowing the cloud chamber to expand. A phantastron delay circuit, with adjustable delay actuated the shutter which fired the flash between 20 and 200 milliseconds after the event. The cloud chamber remained expanded for 15 seconds, then air pressure was again introduced under the diaphragm. When the desired degree of overcompression was attained, the pressure under the diaphragm was auto-



FIG. 3. General experimental arrangement for measuring recoil proton polarization.

[10] E. R. Gaertner and M. L. Yeater, Rev. Sci. Instr. **20**, 588 (1949); also Walker, Bower, and Hadley, *Proceedings of CERN Symposium on High-Energy Accelerators and Pion Physics, 1956* (European Organization of Nuclear Research, Geneva, 1956), Vol. II, p. 40; and N. C. Barford, ibid., p. 35.

TABLE I. Solid angles, cross sections, and counting rates.

| Nominal recoil proton angle | 15° | 30° |
|---|---|---|
| Target to counter 5 distance | 100 cm | 67 cm |
| Solid angle of counter 5 | $45 \times 10^{-4}$ sterad | $102 \times 10^{-4}$ sterad |
| Expected number of protons scattered into counter 5 per $10^6$ incident pions | 15 | 16 |
| Actual average recoil angle | $15.1° \pm 1.0°$ | $30.8° \pm 1.4°$ |
| Average energy of proton at collision with carbon | 102 Mev | 68 Mev |
| Estimated elastic cross section for $p$-$C$ scattering to miss the AC counter | 105 mb | 224 mb |
| Number of protons necessary to enter counter 5 for one acceptable proton-carbon scattering | 69 | 32[a] |
| Expected rate of obtaining the required events | 1 per $4.6 \times 10^6$ pions | 1 per $2.0 \times 10^6$ pions |
| Actual triggering rate | 1 per $0.6 \times 10^6$ | 1 per $0.25 \times 10^6$ |
| Total useful events | 344 | 439 |

[a] The width of the AC counter for the 30° arrangement was $4\frac{1}{2}$ inches.

matically regulated to allow the cloud chamber to return to equilibrium. The cyclotron beam was then turned on and the chamber was ready for the next expansion.

The scattering events were viewed by a prism-mirror arrangement that produced two views side by side on 35-mm film with the use of one lens and shutter. The two stereoscopic views make an effective angle of 11° with the center vertical line to the cloud chamber. The illumination was provided by a 2400 watt-sec discharge through a half-silvered 12-inch long flash tube. The light was focused by two cylindrical Lucite lenses creating a parallel light beam at 90° to the camera direction.

The alignment of the counters 4 and 5 with respect to the hydrogen target was accomplished by optical means. Once picture taking commenced, the cloud-chamber conditions were monitored in the experimentalists' area. The cloud chamber was enclosed in an air-conditioned room which maintained constant temperature to within ±2 F°. It was necessary to check the track conditions about twice each hour and adjust the expansion ratio accordingly. Preliminary scanning of the pictures was done while data was being accumulated so as to detect and quickly correct any abnormalities which might occur in the chamber operation.

## 4. Counting Rates

A total of 15 000 cloud chamber photographs was taken containing about 1000 useful events. The primary contributions to the triggering rate of the chamber came from protons inelastically scattered in carbon and from protons which stopped in the back wall of the chamber, in counter number 5 or in the carbon. The number of pictures taken because of accidental triggerings of the chamber was negligible. Solid angles and counting rates are summarized in Table I.

The meson beam intensity was 5000 pions per second. Thus, for the 15° recoil angle, one would expect a required double scattering event to occur every 15 minutes. Of the scatterings which were obtained, approximately two out of every three had to be discarded during the projection and measurement for failure to satisfy certain criteria explained in the following section. The counter 3 was quite effective in reducing the number of photographs triggered by mesons scattering in the hydrogen. With an empty target, no triggers occurred for $50 \times 10^6$ incident pions.

## III. MEASUREMENT OF CLOUD-CHAMBER PHOTOGRAPHS

The analysis of the pictures was performed by means of stereoscopic projection of the tracks on a suitable arrangement of movable planes. Attached to these planes were the necessary scales and other devices needed to perform the measurements. A detailed description of the apparatus is given by Ashkin et al.[11] With this apparatus the following measurements were made: (1) Recoil proton angle with respect to the incident pion beam (the proton energy is a steep function of this angle). (2) Position of the proton scattering in the carbon plate. This measurement determines the proton energy loss in the carbon and hence the energy of the proton-carbon scattering. (3) The polar and azimuthal angles of the proton scattered by the carbon, where the azimuth is measured from the direction of polarization of the incident proton. (4) A judgment of the degree of elasticity of the proton-carbon scattering. Experimental polarization data exists only for scatterings that are no more than 10-Mev inelastic. An attempt was made to select events in this region. (5) A determination that the event could be accepted without bias. The event was essentially reflected about the plane of polarization, thus creating the same event for a polarization of opposite sign. Details of this procedure are given below.

The incident proton track was checked for straightness and origin. Models of the hydrogen container and of counter number 5 were used to ascertain if the track passed through the counter and originated from the hydrogen target. The position of the scattering was noted for the purpose of determining the energy of scattering.

The direction of polarization of the recoil proton is perpendicular to the plane containing the incident pion and recoil proton. For each event this plane was determined during projection with the help of the recoil proton track and a beam of light arranged to have the same direction relative to the apparatus as the incident meson beam. The planes containing the incident and the scattered proton tracks were arranged to bring the tracks in best focus. Then the polar and azimuthal

---

[11] Ashkin, Kunze, and Romanowski, Atomic Energy Commission Report NYO-2233 (unpublished).
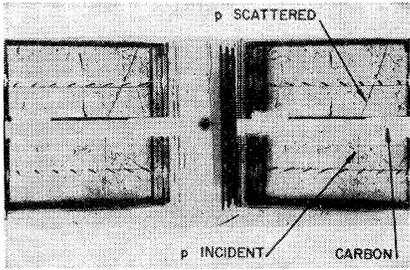
FIG. 4. Typical cloud-chamber photograph of a scattered recoil proton. The band across the center of the photograph is the carbon plate scatterer.

scattering angles and proton recoil angle were measured. To the measured values of angles analytical corrections were applied for the downward displacement of the gas in the cloud chamber caused by its expansion between the time the proton passed through the chamber and the time the track was photographed.

After focusing a scattering event it was necessary to determine if the scattering in carbon was elastic or inelastic. The carbon polarization data[12] includes the elastic scattering or inelastic scattering leading to the 4.4-Mev and the 9.6-Mev excited states of carbon. Beyond the 9.6-Mev level the cross section dips sharply rising again for inelastic scattering with energy loss greater than 20 Mev.[13]

In order to learn about the track densities as a function of energy, protons degraded in energy to 105 Mev, 75 Mev, and 60 Mev were photographed in the chamber for various expansion ratios. There were no visible differences in tracks obtained from the 105-Mev and 75-Mev protons. However tracks produced by 105-Mev and 60-Mev protons differed noticeably in density.

For the 15° recoil protons the average energies of the incident and scattered protons were 114 Mev and 92 Mev, respectively. It is therefore possible that we have included in the 15° measurement some protons which originate in inelastic scatterings leaving the carbon nucleus with an excitation energy greater than 20 Mev. The proton polarization for such scatterings has not been measured. However, we expect only a small error on this account since the scattering cross section for such events[12,13] is small for the angular range below 25° where most of our scatterings lie.

For the 31° recoil protons the average energies of the incident and scattered protons were 86 Mev and 50 Mev, respectively. In this case it was easier to rule out the inelastic events.

Since the carbon analyzer operates by having a propensity to scatter polarized protons more in one direction than into the opposite direction, it is important that the equipment does not discriminate between either direction. If the geometry permitted an event

$(\theta, +\phi)$ to be recorded, but rejected the opposite event $(\theta, -\phi)$, a bias would be introduced. In the experiment the direction of the proton polarization varied with respect to a fixed AC counter causing it to have different geometrical efficiencies for rejection of up and down scatterings, therefore creating a bias. To eliminate such a bias, the scattered track was extended on to the plane of the AC counter and then reflected in the azimuthal angle. If either track passed through the counter the event was discarded. A photograph of a typical scattering event is shown in Fig. 4.

## IV. ANALYSIS OF DATA

For a proton beam of polarization $P$ scattered from carbon, the probability of a scattering occurring at a given polar angle $\theta$ and azimuthal angle $\phi$ ($\phi$ is measured from the plane of polarization) is, according to Eq. (1):

$$P(\theta,\phi,E)d\Omega = A^{-1}[d\sigma(\theta,E)/d\Omega]$$
$$\times [1+PP_c(\theta,E) \sin\phi]d\Omega. \quad (2)$$

To obtain normalized probability, the factor $A$ is obtained by integrating Eq. (2) over all solid angles not excluded by the AC counter. By the reflection criterion used to prevent any bias (Sec. III), the excluded region is made to include the "reflection" of the AC counter (around $\phi=0$) as well. As a result the integration becomes symmetrical about $\phi=0$, and the (unknown) polarization, $P$, is no longer contained in the normalization factor.

Each measured event will have a probability of occurrence which will be a function of the initial recoil proton polarization, $P$. The total probability $L$ of obtaining all the events that were measured will be the product of the individual probabilities for these events. One would expect that the actual recoil proton polarization would be close to the value of $P$ making this probability a maximum. We have accordingly maximized the expression

$$L = \prod_{i=1}^{i=n} [1+PP_c(\theta,E)_i \sin\phi_i], \quad (3)$$

omitting a normalization factor independent of $P$. The curves of $L$ as a function of $P$ shown in Fig. 5 were calculated with an IBM-650 computer. See Appendix I for further discussion of the maximum likelihood method as applied to this problem.

We have adopted a sign convention which makes the polarization of the recoil proton positive in the direction of the vector cross product between the incident pion momentum and the recoil proton momentum. In accordance with the experiments[14] which determine the sign of $P_c(\theta,E)$, protons with positive polarization will be preferentially scattered upward as shown in Fig. 2.

[12] J. M. Dickson and D. C. Salter, Nuovo cimento 6, 235 (1957); also Dickson, Rose, and Salter, Proc. Phys. Soc. (London) A68, 361 (1955).
[13] K. Strauch and F. Titus, Phys. Rev. 103, 200 (1956).

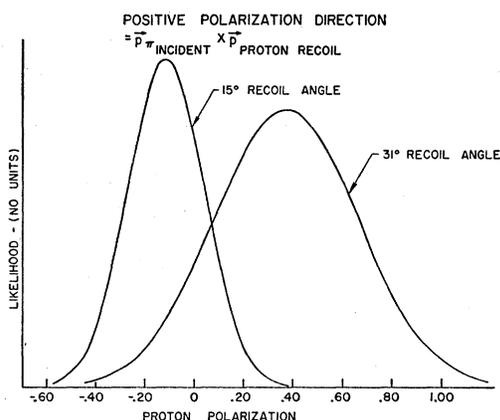[14] L. Marshall and J. Marshall, Phys. Rev. 98, 1398 (1955); also M. T. Brinkworth and B. Rose, Nuovo cimento 3, 195 (1956).

FIG. 5. Maximum likelihood graphs for proton recoil angles of 15° and 31°.

Taking $P_c(\theta,E)$ positive requires that upward scatterings correspond to positive values of $\sin\phi$.

$P_c(\theta,E)$ has been measured for laboratory angles from 5° to 30° and at several different energies between 56 and 135 Mev at Harwell by Dickson and Salter.[12] They used a NaI counter to separate the elastic and inelastic scattering to the 4.4-Mev and 9.6-Mev levels. Since the protons corresponding to these levels are not distinguishable in the cloud-chamber pictures, the Harwell data was combined to obtain an effective polarization given by the curves in Fig. 6. For each scattering event, $P_c(\theta,E)$ was obtained by interpolation. Besides using curves drawn through the centers of the experimental points, a set was drawn through the top of the error, and another set through the bottom. Each of these sets was used for the 15° recoil data, and the final polarization results differed by less than 0.04. Though the Harwell data extended only to 30°, the curves were extrapolated to 35° for those energies around 100 Mev, and to 40° for those near 70 Mev (these curves are relatively flat). The maxima were scaled according to a $1/E$ law.

For those events in which the scattering appears to occur in the scintillant, the possibility of a $p$-$p$ scattering must be considered. The polarization effects in $p$-$p$ scattering have been measured by various investigators[15] and this data and the carbon data were used to calculate the relative efficiency of the scintillant as a polarization analyzer compared to pure carbon.

## V. ERRORS

The polarization measurement is done essentially by determining the number of up scatterings $vs$ the number of similar type down, and weighing these events according to the effective analyzing power of each. Of the systematic errors that might be present, those which would add or subtract equally to the up and

down events would be of far less concern than those that would affect the up events differently from the down. The former type are not to be ignored completely, for they will affect the statistical error and slightly alter the magnitude of the result. The latter type of errors will greatly affect the magnitude and, in extreme cases, even the sign of the result. In the following discussion these errors will be classified as symmetrical and asymmetrical, respectively, with particular attention given to the latter.

### (A) Errors During Accumulation of Data

(1) *Misalignment of the AC counter (asymmetrical).*— Such a misalignment would cause more small angle up events to be recorded than the similar type down events, or conversely. The AC counter position was reproduced to within a fraction of a degree for the projection arrangement. Reflected events which hit the AC were rejected.

(2) *Misalignment of the cloud-chamber effective recoil angle (symmetrical).*—With the optical aligning system used, it is believed that the correct mean recoil angle was known and reproduced to within $\frac{1}{2}°$.

(3) *Cloud-chamber illumination or sensitivity asymmetries (asymmetrical).*—The cloud chamber was found to produce tracks of equivalent photographic density over a range from $\frac{1}{2}$ in. below to $\frac{1}{2}$ in. above the cloud-chamber counter. Steep scattered tracks that went beyond these limits began to fade on the photographs. The sensitivity was checked by photographing a col-
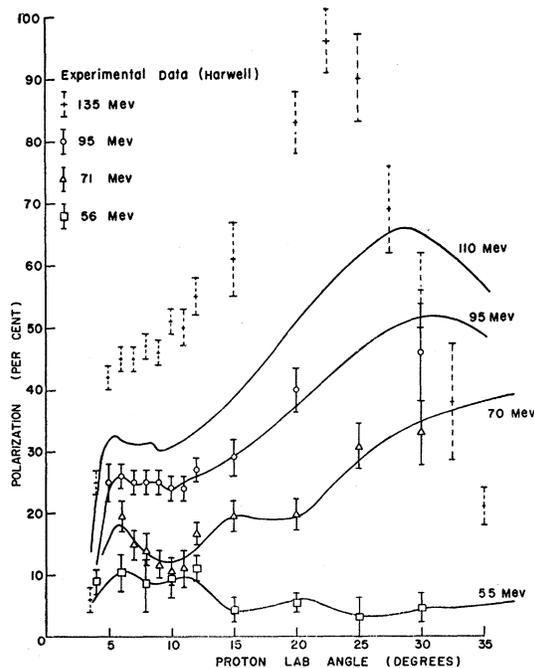


FIG. 6. Polarization of protons scattered from carbon. Experimental points are those of Dickson and Salter.[12]

[15] O. Chamberlain *et al.*, Phys. Rev. **83**, 923 (1951); Baskir, Hafner, Roberts, and Tinlot, Phys. Rev. **106**, 564 (1957); also J. M. Dickson and D. C. Salter, Nature **173**, 946 (1954).

limated beam at various positions in the chamber. It is believed that no events were missed because of illumination or sensitivity asymmetries. All the film was scanned at least once in a viewer, and a second time during projection and measurement. Failing to detect an event would be extremely unlikely.

## (B) Errors During Projection

(1) *Examination of tracks to determine if scattered.*— All of the pictures were projected except those that, on the rough examination in the viewer, definitely contained no proton or a proton which stopped in the carbon. Some small angle scatterings would appear straight in one dimension. However, there was no uncertainty in identifying these as scatterings during projection.

(2) *Error in the high cutoff angle (asymmetrical).*— Scatterings greater than $35\frac{1}{2}°$ for the 15° recoil and $40\frac{1}{2}°$ for the 31° recoil arrangements were arbitrarily eliminated from consideration. Only a few events occurred near these large angles. A $\frac{1}{2}°$ asymmetrical error in these cutoff angles between the up and down events would have little effect on the final result.

(3) *Error in the incident pion direction (asymmetrical).* —The pictures of the direct meson beam did not show any obvious departures from a parallel beam. The two monitor counters and the target were spaced sufficiently so that a meson could not pass through all three unless it made an angle of 2° or less with the center line. It is thought that departures from the center line of the beam would be random.

(4) *Errors in the angle measurements.*—The errors in the measurement of the angles of the scatterings introduce a complex error into the result. All of the data was measured at least twice and the results are given in Table II. The differences between the two sets of measurements would be caused primarily by differences in the judgment of the observers performing the measurements. The finite thickness of the tracks and the slight distortions, due to the motion of the gas of the cloud chamber, make a completely unambiguous determination of the scattering angles and position of the scattering in the carbon practically impossible. Most systematic error in judgment would be expected to be symmetrical, such as measuring the angles too large. The same error would be made on the down scatterings as on the up scatterings. A systematic asymmetrical error would be introduced by a projection apparatus that had misaligned planes. The planes appeared to be aligned and accurate to within $\frac{1}{4}°$. It is believed that they could not contribute a significant error. The average deviation of the polar angle measurements due to judgment was $\frac{1}{3}°$.

The track displacement was symmetrical, so as to always move the observed track nearer to the horizontal. Any small error in these displacement correc-

TABLE II. Proton polarizations from two scannings of acceptable events.

| | Initial measurement | Remeasurement |
|---|---|---|
| *15° recoil angle results* | | |
| Number of events accepted | 346 | 343 |
| Mean recoil angle | 15.2° | 15.1° |
| $(P_c \sin\phi)_{average}$ | 0.318 | 0.324 |
| Polarization | $-0.15\pm0.16$ | $-0.12\pm0.16$ |
| | | |
| *31° recoil angle results* | | |
| Number of events accepted | 446 | 431 |
| Mean recoil angle | 30.7° | 30.9° |
| $(P_c \sin\phi)_{average}$ | 0.136 | 0.138 |
| Polarization | $+0.35\pm0.29$ | $+0.39\pm0.29$ |

tions would, therefore, not alter the magnitude of the result appreciably.

Rejection or acceptance of the events in which the direct or reflected scattering came close to the AC was a delicate task. All of these events were very carefully remeasured.

In general, the same observer did not perform more than one of the measurements of any particular event (there was overlapping, but on less than 50% of the events). The results of the two measurements is quoted for the final result. Because of this uncertainty due to the angle measurements, an additional error of 0.02 should be added to the statistical spread.

## VI. MEASUREMENT OF A KNOWN POLARIZATION

Asymmetries in the experimental arrangement may be undetectable by ordinary visual inspection. Either the apparatus used for obtaining the pictures or the projection system could be at fault. It was thought desirable to measure the known polarization of a beam of protons of equivalent energy, using a similar experimental arrangement as that encountered in the main experiment. The result of such a measurement, if consistent with the known polarization value, cannot necessarily serve as a calibration for the cloud chamber, unless the statistical errors of the measurement are very small. The result could, however, enhance the faith in the validity of the main experimental results, and indicate that no serious asymmetries exist.

The identical experimental arrangement, as used in the pion beam, was placed in the unpolarized proton beam of the cyclotron. Lithium hydride absorber reduced the proton energy from 440 to 140 Mev. The selecting magnet bent the 140-Mev protons about 24° into the monitor counter telescope. The protons were scattered by a 1-cm thick carbon target instead of liquid hydrogen. A counter was placed at the target to better define the recoil proton beam entering the cloud chamber and thus increase the efficiency of obtaining useful scattering events. Half of the data were accumulated with the protons scattering up into the cloud chamber, the other half with downward scattered

TABLE III. Polarization measurements of protons
with known polarization.

|  | Chamber level | Chamber up | Chamber down |
|---|---|---|---|
| First scattering mean angle | 0° | 20.6° | 20.2° |
| Number of events | 159 | 86 | 119 |
| $(P_c \sin\phi)_{average}$ | 0.406 | 0.393 | 0.387 |
| Polarization | +0.13±0.18 | +0.84±0.25 | +0.38±0.20 |

Combined result of chamber up and chamber down:
Polarization = +0.55±0.16

protons, the up and down angles of the cloud chamber being the same in both cases. The polarization of the protons entering the cloud chamber was known from the average energy and angle of the first scatterings. A mean angle of 20° was chosen, and the mean energy of the first scattering was (133±7) Mev. The average polarization under these conditions, including the scattering to the 4.4-Mev and 9.6-Mev levels as measured at Harwell,[12] is +0.80±0.05. The mean energy of the second scatterings in the cloud-chamber carbon plate was 115 Mev.

The incident proton beam was reduced to several thousand per second over 7 in.[2] The pictures with double scattering events were carefully measured, and later remeasured.

The chamber was then leveled into the direct proton beam which was assumed to be unpolarized. The beam intensity was again reduced and about 30% of the cloud-chamber pictures were good events. The results of these three measurements are given in Table III. The chamber down result does not agree with the Harwell result. The cause of the discrepancy can be attributed partially to the fact that many of the scatterings into the cloud chamber may have been inelastic beyond the 9.6-Mev level. Because of the high incident energy (133 Mev), 20- to 40-Mev inelastic scatterings would be impossible to distinguish visually from elastic scatterings. Therefore, the measured polarization may have included lower polarization contributions from the more inelastic levels. A result of somewhat less than 80% would be expected.

We prefer to interpret the results as indicating that the cloud chamber and measuring procedure do not suffer from any serious asymmetry. It was not considered feasible to continue the proton beam measure-

TABLE IV. Mean proton polarization obtained from
the measured and remeasured values.

|  | 15° recoil angle | 31° recoil angle |
|---|---|---|
| Average recoil angle | 15.1°±1.0° | 30.8°±1.4° |
| Number of events | 344 | 438 |
| Mean energy of carbon scattering | 102 Mev | 68 Mev |
| Polarization | −0.13±0.16 | +0.37±0.29 |

TABLE V. Mean proton polarization for 15° proton recoil for
chamber in the lowered and raised position.

| 15° recoil angle | Chamber up | Chamber down |
|---|---|---|
| Number of events | 144 | 200 |
| Mean recoil angle | 15.4° | 14.9° |
| Polarization | +0.03±0.23 | −0.25±0.21 |

ments. The efficiency of obtaining events was poor because a recoil counter could not be used as an aid to recording only good events.

## VII. RESULTS

The polarization measurements were made at two recoil proton angles with mean values of 15.1°±1.0° and 30.8°±1.4°. The angular spreads are standard deviations computed from the measured recoil angles for all of the events. The results are listed in Table IV, and represent the mean values of the initial measurements and the remeasurements. The larger error for the 31° result is caused by the poorer analyzing power of the carbon at the lower scattering energy. The errors are the statistical error of the maximum likelihood solution and do not include an uncertainty resulting from the inaccuracies of the scattering angle measurements. This additional uncertainty amounts to about ±0.02.

The 15° data were obtained with the cloud chamber both in the raised and lowered positions so as to compensate for any bias inserted by the cloud chamber and associated apparatus. Because of space limitations similar procedure could not be followed for the case of 31° recoil protons. These results, listed in Table V, were in agreement within the experimental errors. The values listed are the mean of the initial measurement and the remeasurement.

The sensitivity of the data to the carbon polarization curves was tested by changing these curves with respect to the Harwell experimental points. The "mean" curves are those used for the results in Table IV and are shown plotted approximately through the centers of the experimental points in Fig. 6. "High" and "low" curves were drawn through the tops and bottoms of the experimental errors, respectively. The results, using altered curves, are shown in Table VI for the initial measurement only. The value for Mean $P_c$ will not necessarily be between the values for High and Low $P_c$ because of the complicated shapes of these three sets of curves.

TABLE VI. Proton polarization at 15° recoil for different
values of carbon polarization.

| 15° recoil angle | High $P_c$ | Mean $P_c$ | Low $P_c$ |
|---|---|---|---|
| $(P_c \sin\phi)_{average}$ | 0.359 | 0.318 | 0.286 |
| Polarization | −0.105±0.140 | −0.145±0.160 | −0.135±0.177 |

TABLE VII. Phase-shift sets used in calculation of
proton polarization and $M$ values.

| | Fermi (i) | Fermi (ii) | Yang (i) | Yang (ii) |
|---|---|---|---|---|
| *Phase shifts* | | | | |
| $\alpha_3$ | $-14.5°$ | $-18°$ | $-16.5°$ | $-17.8°$ |
| $\alpha_{33}$ | 112 | 112 | 139.6 | 142.3 |
| $\alpha_{31}$ | $-5$ | 0 | 253 | 257.4 |
| $\alpha_1$ | 15 | $-8.5$ | 11.6 | $-9.5$ |
| $\alpha_{13}$ | $-5$ | 11.5 | $-3.5$ | 9.6 |
| $\alpha_{11}$ | 7 | 3 | 1.6 | 8.2 |
| *M values for scattering processes* | | | | |
| $M(\pi^+ \pi^+)$ | 4.92 | 5.22 | 5.09 | 4.44 |
| $M(\pi^- \pi^-)$ | 8.76 | 8.71 | 9.88 | 11.88 |
| $M(\pi^- \pi^0)$ | 6.13 | 9.20 | 6.77 | 11.82 |
| Sum | 19.81 | 23.13 | 21.74 | 28.14 |
| *M for polarization* | 0.58 | 15.47 | 30.65 | 2.43 |
| Total $M$ | 20.39 | 38.60 | 52.39 | 30.57 |

## VIII. CONCLUSIONS

The results listed in Table IV are plotted in Fig. 1.
The phase-shift sets corresponding to each curve of
that figure are listed in Table VII along with the values
of a quantity $M$ measuring the quality of the over-all fit
to the two elastic cross sections, the charge exchange
cross section, and the polarizations. $M$ represents the
sum of the squared deviations between the measured
values and the values computed from the phase shifts,
in units of the experimental error. The cross-section
data are from the paper by Ashkin *et al.*[2]

The phase-shift analysis performed in reference 2 was
preliminary and did not necessarily represent the best
fit to the existing experimental data. A more extensive

phase-shift analysis was recently performed by Chiu
and Lomon.[16]

Without the inclusion of the polarization results, the
$M$ values are about the same for each of the four sets
of phase shifts. It appears that the polarization results
have definitely excluded the two phase shift sets
Fermi (ii) and Yang (i). Of the other two sets, the
Fermi (i) seems to be favored, though preference for it
over the Yang (ii) cannot be established conclusively
on the basis of the present experimental information
alone.

Experimental elimination of the Fermi (i)-Yang (ii)
ambiguity is possible through a sufficiently accurate
measurement of the polarization at appropriate angles.
However, further reduction of the experimental error
of the 31° point is practically not feasible with our
present beam intensity. A measurement at a recoil
angle of 50° could not be made with the present experi-
mental equipment because of the very low energy
(53 Mev) of the recoil proton.

## APPENDIX I. NORMALIZATION OF THE MAXIMUM LIKELIHOOD METHOD FOR THE MEASUREMENT OF POLARIZATION

The probability of occurrence of an event, $i$, is given
by Eq. (1')

$$p_i d\Omega_i d(loc)_i = \frac{[d\sigma(\theta,E)/d\Omega_i](1+PP_c \sin\phi)_i G_i(\theta,\phi,loc)d\Omega_i d(loc)_i}{\int\int\limits_{\substack{\text{all admissible angles and locations}}} [d\sigma(\theta,E)/d\Omega](1+PP_c(\theta,E) \sin\phi)G_i(\theta,\phi,loc)d\Omega d(loc)} \qquad (1')$$

$G_i(\theta,\phi,loc)$ is a geometrical factor, determined by the
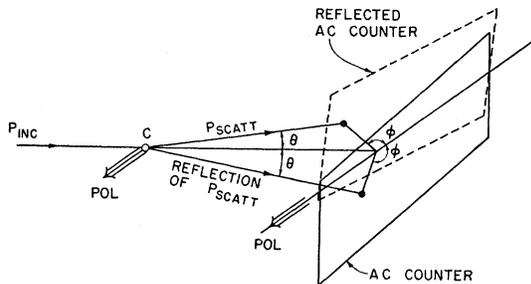location of the event in the carbon plate, the size of the



FIG. 7. Diagram showing the reflection criterion for selecting or
rejecting appropriate events for the final analysis.

cloud chamber and AC counters, the carbon thickness,
and other variables, all of which we shall denote as
"location" variables.

The denominator must be independent of $P$ for the
maximum likelihood method to be easily employed.
Thus, the integration over $\phi$ must be symmetrical about
$\phi=0$. The integration is not performed over the region
of the AC counter [inadmissible region $G(\theta,\phi,loc)=0$],
and therefore must not be performed over the region
of an AC counter reflected about the line $\phi=0$ (direction
of polarization, $P$). Events which would occur in the
region of the reflected AC counter must be excluded
from consideration (Fig. 7). In practice, it is easier and

[16] H. Y. Chiu and E. L. Lomon, Ann. Phys. 6, 50 (1959).

equivalent to exclude the events which, upon reflection, would hit the unreflected AC counter. If the above conditions are met, each event will have a different normalizing factor, but these factors will be independent of $P$. The true likelihood of all of the events will then be expressed by (2′)

$$L = (\text{constant}) \prod_{i=1}^{n} (1 + PP_c(\theta, E)_i \sin\phi). \qquad (2')$$

About 30% of the scatterings were discarded because they did not satisfy this reflection criterion.

### APPENDIX II. $\pi^- - p$ POLARIZATION FORMULA

The derivation of the polarization formula for pion-proton scattering, in which only $s$ and $p$ orbital angular momentum states contribute, is given in reference 6. The resulting formula is given below.

If a normal right-hand set of axes, $x$, $y$, $z$, are defined, with the incident pion momentum along the $+z$ axis, and the recoil proton momentum in the $(x,z)$ plane with a component in the $+x$ direction, the polarization will be given by Eq. (1″),

$$P = \frac{p(+y \text{ direction}) - p(-y \text{ direction})}{p(+y \text{ direction}) + p(-y \text{ direction})}, \qquad (1'')$$

where the $p$'s are probabilities of the spin being along the direction specified.

For the case of $\pi^-$ mesons scattered from protons, there are two isotopic spin states, $T = \frac{3}{2}$ and $T = \frac{1}{2}$, and three total angular momentum states, $j = \frac{3}{2}, \frac{1}{2}$ for $p$ waves, and $j = \frac{1}{2}$ for $s$ waves. There are thus six phase shifts. The probability of spin-flip scattering will, in general, be different than for non-spin flip scattering, thus giving rise to a polarization,

$$P = i\frac{\sin\theta(X^*Z - XZ^*) + \sin\theta \cos\theta(Y^*Z - YZ^*)}{|X + Y\cos\theta|^2 + |Z\sin\theta|^2}, \qquad (2'')$$

where $X = a_3 + 2a_1$, $Y = (2a_{33} + a_{31}) + 2(2a_{13} + a_{11})$, and $Z = (a_{31} - a_{33}) + 2(a_{11} - a_{13})$. The $a_{ij}$ are the $p$-wave scattering amplitudes, the $a_i$ the $s$-wave amplitudes. In terms of the phase shifts, $\alpha_{ij}$,

$$a_{ij} = (1/2i)[\exp(2i\alpha_{ij}) - 1].$$

---

# Thirring Model with Variable Interaction

F. L. SCARF*
*CERN, Geneva, Switzerland*
(Received June 15, 1959)

The Thirring model is solved with a variable coupling constant, $\lambda = \lambda_0 f(x,t)$. It is found that the infrared divergence is eliminated if $f$ tends to zero along the past light cone. The $S$ matrix is no longer diagonal in the physical particle representation and is generally not well-defined in the sense of Haag's theorem. The ordered, renormalized Heisenberg operators for $\psi$, $\psi \psi^*$ are computed and production processes are analyzed by examining matrix elements.

## 1. INTRODUCTION

THE two-dimensional relativistic model introduced by Thirring[1] has served as a valuable tool for the exploration of the structure of quantum field theory. There are, however, two aspects of the original model that limit its usefulness. Because of the small number of dimensions, an infrared divergence is present in the wave function renormalization constant, and therefore some renormalized products of a finite number of field operators do not exist. Furthermore, the $S$ matrix is diagonal in the physical particle representation so that creation of matter does not occur.

In this paper we discuss a modified, but still soluble, version of the Thirring model with variable coupling,

$\lambda = \lambda_0 f(x,t)$. In general, the $S$ matrix is not diagonal and for a large class of functions $f(x,t)$ no infrared divergence appears. Consequences of adiabatic variations or discontinuous changes in $\lambda$ may also be examined with the extended model.

Section 2 contains a discussion of the equations of motion, their operator solutions and the construction of state vectors. Although energy and momentum are not conserved, the particle-number operators remain diagonal. It is shown that the $S$ matrix is identical to the $U$ matrix for certain forms of $f$, suggesting that the former is ill-defined in the sense of Haag's theorem.

In Sec. 3, the Heisenberg operators for $\psi$ and $\psi\psi^*$ are ordered and renormalized by using configuration space techniques which are related to Glaser's methods for the original model. Matrix elements of these operators are employed to discuss the elementary production processes in Sec. 4, and the conclusions are summarized

---

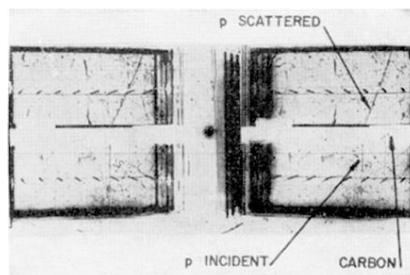[1] W. E. Thirring, Ann. Phys. **9**, 91 (1958).

FIG. 4. Typical cloud-chamber photograph of a scattered recoil proton. The band across the center of the photograph is the carbon plate scatterer.